

Semiconducting Polymer Dots Doped with Europium Complexes Showing Ultranarrow Emission and Long Luminescence Lifetime for Time-Gated Cellular Imaging**

Wei Sun, Jiangbo Yu, Ruiping Deng, Yu Rong, Bryant Fujimoto, Changfeng Wu, Hongjie Zhang, and Daniel T. Chiu*

Polymer dots (Pdots) have emerged as a new type of nanoprobe that have a wide range of applications in fluorescence imaging and biosensing.^[1] Compared to small fluorescent dyes and quantum dots (Qdots), Pdots possess larger absorption cross-sections, faster emission rate, and better photostability.^[2,3] These properties have enabled them to be used for single-particle/carrier tracking over long periods of time.^[4,5] Moreover, the full width at half maximum (FWHM) of the emission band of Pdots can be as narrow as approximately 40 nm, an important feature for multiplexed assays.^[2,6] In addition, the diameter of Pdots can be tuned to be below 10 nm, which makes them excellent nanoprobe for targeted subcellular labeling experiments.^[7] The applicability of the superior optical properties of Pdots has also been demonstrated for tumor imaging in animals.^[8]

Organic europium complexes are bright, luminescent materials that have been used for applications such as making organic light-emitting diodes^[9] and bioimaging.^[10–12] Eu complexes have several merits not found in other organic fluorescent dyes: 1) their luminescence emission is usually line-like with the FWHM smaller than 10 nm; 2) the emission spectra are less affected by the environment, such as fluctuations in oxygen concentration, than emission spectra of other heavy metal complexes;^[13] 3) they have a large Stokes shift; 4) they have long luminescence lifetime.^[14]

Various kinds of luminescent nanoparticles have been developed by doping Eu complexes into a matrix, such as silica or a nonfluorescent polymer.^[15–19] But because of self-quenching among Eu complexes, the loading ratio of Eu complexes into the matrix has been kept to low levels to improve the quantum yield (QY).^[15,20] Therefore, for these types of fluorescent nanoparticles, the total brightness still has been limited.

Our recent study has proved that Pdots can act as excellent host matrices and good energy-transfer donors for small organic dyes and inorganic nanoparticles.^[21–23] Here, we doped Eu complexes into Pdots made of the semiconducting polymer poly(9-vinylcarbazole) (PVK). Not only did PVK function as a host matrix to disperse the Eu complexes and reduce the self-quenching of the Eu complexes, it also acted as an efficient fluorescence energy donor with a large absorption cross-section to transfer energy to the Eu complexes. The Eu complex/PVK Pdots had ultranarrow red fluorescence emission and showed much higher emission brightness than pure Eu complex nanoparticles. In addition, the long luminescence lifetime of the Eu complex was carried over to the Eu complex/PVK Pdots; we demonstrated this long luminescence lifetime was useful in particle differentiation and cell imaging with a greatly improved signal-to-noise (S/N) ratio.

The method to prepare Eu complex/PVK Pdots was based on nanoprecipitation^[24] as depicted in Scheme 1 b. Here, an Eu complex (Eu15F or EuDNM) was mixed with the semiconducting polymer PVK and block copolymer PS-PEG-COOH in THF. After being injected into water, the polymer chains collapsed to form nanoparticles and embedded Eu complexes inside the nanoparticles. The sizes of Eu15F/PVK and EuDNM/PVK Pdots were measured by using dynamic light scattering (DLS) to be smaller than 20 nm in diameter, which were confirmed by high-resolution transmission electron microscopy (TEM) images (Figure 1 a–d).

Here, PVK was chosen as the host matrix, because its emission spectrum overlapped with the excitation spectra of Eu15F and EuDNM (Figure 1 e,f). The spectral overlap made it possible for Förster resonance energy transfer (FRET) to take place between the donor PVK and the acceptor Eu complexes inside the Eu complex/PVK Pdots. For example, as shown in the emission spectra (Figure 1 e), the emission peak of the pure PVK Pdots was centered at 398 nm when the excitation wavelength was 342 nm; when the Eu complex/PVK Pdots were excited at 342 nm, a red-shifted emission was observed centered at approximately 612 nm. In addition, with

[*] Dr. W. Sun,^[†] Dr. J. B. Yu,^[†] Dr. Y. Rong, Dr. B. Fujimoto, Prof. D. T. Chiu

Department of Chemistry, University of Washington
Seattle, WA 98195 (USA)
E-mail: chiu@chem.washington.edu

Dr. R. P. Deng, Prof. H. J. Zhang
State Key Laboratory of Rare Earth Resource Utilization, Changchun
Institute of Applied Chemistry, Chinese Academy of Sciences
Changchun 130022 (China)

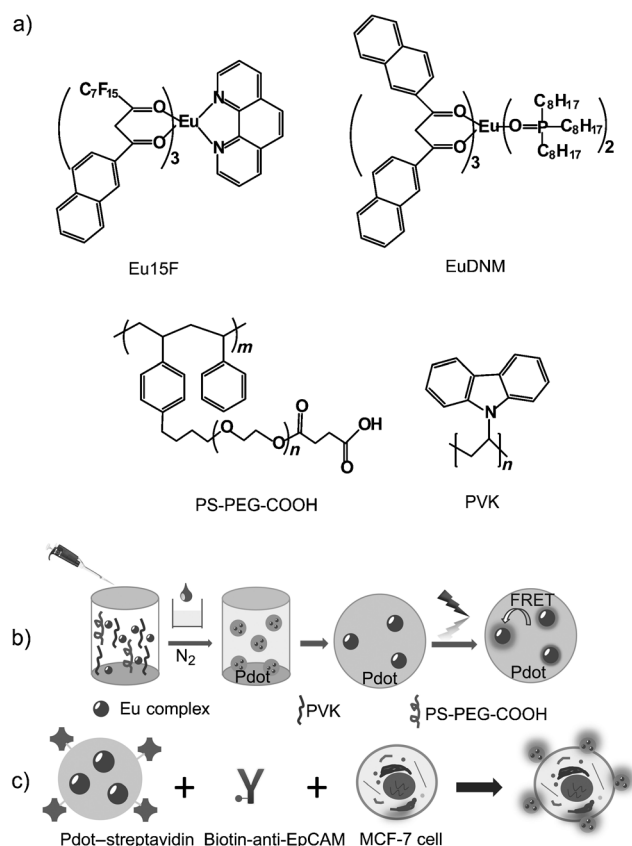
Prof. C. F. Wu
State Key Laboratory on Integrated Optoelectronics
College of Electronic Science and Engineering, Jilin University
Changchun, Jilin 130012 (China)

[†] These authors contributed equally to this work.

[**] D.T.C. gratefully acknowledges support for this research from the National Institutes of Health (NS052637 and GM085485), the Life Sciences Discovery Fund, and the University of Washington. R.P.D. and H.J.Z. are grateful to the financial aid from the National Natural Science Foundation of China (91122030) and National Natural Science Foundation for Creative Research Group (21221061).



Supporting information for this article is available on the WWW under <http://dx.doi.org/10.1002/ange.201304822>.



Scheme 1. a) Chemical structures of Eu15F, EuDNM, PS-PEG-COOH, and PVK; b) the preparation procedure of Eu complex/PVK Pdots; c) the procedure for labeling cells by using Eu complex/PVK Pdot-streptavidin bioconjugates.

the increase of emission intensity at 612 nm, the emission intensity at 398 nm (from PVK) dropped significantly even when the ratio of doped Eu complex to PVK was only 20 % (Figure 1g,h). The trend was observed for both Eu15F/PVK and EuDNM/PVK Pdots. Moreover, the emission of the Eu complex/PVK Pdots was very narrow. For pure PVK Pdots, its broad emission covered the range from 350 nm–500 nm; for Eu complex/PVK Pdots, the FWHM of the emission peak (612 nm) was only 8 nm, which is also much narrower than that of most organic dyes and Qdots.

The QY values of the Eu complex/PVK Pdots were also measured at various Eu complex doping ratios. First, pure Eu complex nanoparticles were prepared by injecting Eu complexes dissolved in THF into water. The measured QYs of pure Eu15F and EuDNM nanoparticles were 7.8 % and 5.8 %, respectively. For both Eu complexes at the doping ratio of 60 wt % in the PVK host polymer, the QY increased to be as high as 33.5 % for Eu15F/PVK Pdots and 11.2 % for EuDNM/PVK Pdots. The significant QY enhancement indicated that the self-quenching among Eu complexes inside the Eu complex/PVK Pdots was greatly reduced. We noted that when the doping ratio of the Eu complex reached 80 wt %, the QY of Eu complex/PVK Pdots began to decrease slightly (Figure 1g,h), which was possibly due to concentration quenching. The high doping ratio of Eu complex and

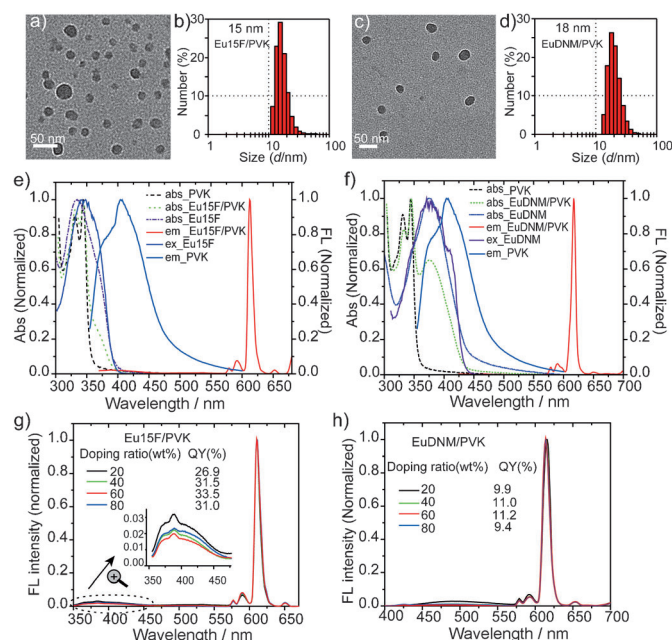


Figure 1. Size and optical property characterization of Eu complex/PVK Pdots. a) High-resolution TEM image of Eu15F/PVK Pdots. b) DLS size distribution histogram of Eu15F/PVK Pdots. c) High-resolution TEM image of EuDNM/PVK Pdots. d) DLS size distribution histogram of EuDNM/PVK Pdots. e) Normalized absorption (abs), excitation (ex), and emission (em) spectra of pure PVK Pdots, Eu15F nanoparticles, and Eu15F/PVK Pdots. All spectra were measured in aqueous solution. f) Normalized spectra of pure PVK Pdots, EuDNM nanoparticles, and EuDNM/PVK Pdots. g) The emission spectra of Eu15F/PVK Pdots with the doping ratio of Eu15F ranging from 20 % to 80 %; the excitation wavelength was 342 nm; QY data and amplified partial emission bands of Pdots are shown in the inset. h) The emission spectra of EuDNM/PVK Pdots with the doping ratio of EuDNM ranging from 20 % to 80 %; the excitation wavelength was 342 nm; QY data of Pdots are shown in the inset.

extinction coefficient of PVK made it possible for the Eu complex/PVK Pdots to have a large absorption cross-section (Table 1), which was in the same order of magnitude as that of other reported Pdots.^[24,25] Because of their high absorption cross-section, doping ratio, and quantum yield, the Eu complex/PVK Pdots exhibited great single-particle brightness. In the Eu complex/polymer^[20] nanoparticles or Eu

Table 1: Summarized photophysical properties of Eu complex/PVK Pdots.

Pdots	Size [nm]	$\sigma^{[a]}$ [$\times 10^{-13}$ cm ²]	$\eta^{[b]}$ [%]	$\tau^{[c]}$			
				A ₁	τ_1 [μ s]	A ₂	τ_2 [μ s]
Eu15F/PVK (40wt %)	15	0.65	31.5	0.09	103	0.15	509
EuDNM/PVK (60wt %)	18	1.20 (0.70 ^[d])	11.2	0.02	38	0.02	202

[a] Absorption cross-section for single particles; [b] absolute luminescence QY (± 0.5 %); [c] luminescence lifetime; A₁ is the amplitude for lifetime τ_1 ; A₂ is the amplitude for lifetime τ_2 . [d] absorption cross-section calculated for a single particle with a size of 15 nm; size refers to the hydrodynamic diameter measured by DLS.

complex/silica^[16,17] nanoparticles reported to date, they may have high quantum yields but the single-particle brightness of these kinds of fluorescent nanoparticles have been low. The doping ratios of Eu complex inside these nanoparticles were usually kept at a low level (smaller than 5 %),^[16,17] and the host materials (silica or latex polymer) are generally transparent in the region of 300–650 nm; these properties do not help to increase the single-particle absorption cross-section. Therefore, our Pdots provided a new way to decrease the self-quenching of Eu complex fluorescence and reach high single-particle brightness.

We recently performed bioconjugation reactions at the surfaces of Pdots successfully and demonstrated the application of Pdot–streptavidin (Pdot–SA) bioconjugates to in vitro targeting of specific cellular components and in vivo tumor targeting.^[24] Similarly, for this work, we attached streptavidin to the Eu complex/PVK Pdots by using the same strategy. The Eu complex/PVK Pdot–streptavidin conjugates successfully labeled the cell surface receptor EpCAM (Scheme 1c). As shown in the flow cytometry results in Figure 2a,b, the

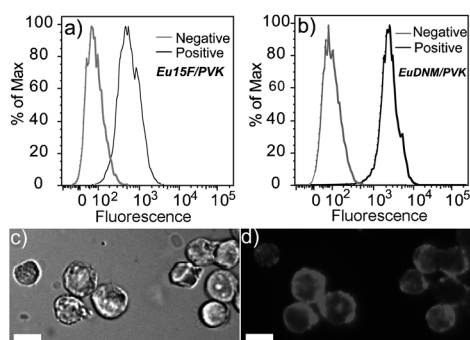


Figure 2. Immunofluorescence labeling of MCF-7 cells with Eu complex/PVK Pdots and flow cytometry measurements. a) Flow cytometry measurements of cells labeled with Eu15F/PVK Pdot–SA; b) flow cytometry measurements of cells labeled with EuDNM/PVK Pdot–SA. In (a) and (b), the gray curve shows the negative control and the dark curve is for the positive sample. On the x axis, the fluorescence emission collected in the PE-Texas Red-A channel is displayed. c) Bright-field image taken by optical microscopy of MCF-7 cells labeled with Eu15F/PVK Pdots. d) Fluorescence image of MCF-7 cells labeled with Eu15F/PVK Pdots. In (c) and (d), scale bar is 20 μm .

positively labeled cells (incubated with Eu complex/PVK Pdot–streptavidin in the presence of the biotinylated primary antibody) were distinctly separated from the negatively labeled cells (incubated with Eu complex/PVK Pdot–streptavidin in the absence of the biotinylated primary antibody). The specific cellular labeling was also confirmed by fluorescence microscopy, because the positively labeled cells emitted very strong red fluorescence (Figure 2c). The flow cytometry results demonstrated that the streptavidin-conjugated Eu complex/PVK Pdots had a high specific labeling efficiency with low nonspecific binding.

From the luminescence lifetime measurements of the Eu complex/PVK Pdots, we found that these Pdots inherited the long luminescence lifetimes of their corresponding Eu complexes. As shown in Table 1, the lifetime of Eu15F/PVK and

EuDNM/PVK Pdots was around 509 and 202 μs , respectively, which were significantly longer than the 17 ns lifetime of pure PVK Pdots. It also indicated that there was efficient FRET between the PVK polymer and the Eu complex inside the Pdots. The unique property of having a long luminescence lifetime distinguishes Eu complex/PVK Pdots from other nanoparticles emitting red fluorescence. For example, both Eu15F/PVK Pdots and commercial red fluorescent nanoparticles (R300 NPs) had a strong emission at 612 nm (Figure 3a). Owing to the spectral overlap, the two types of

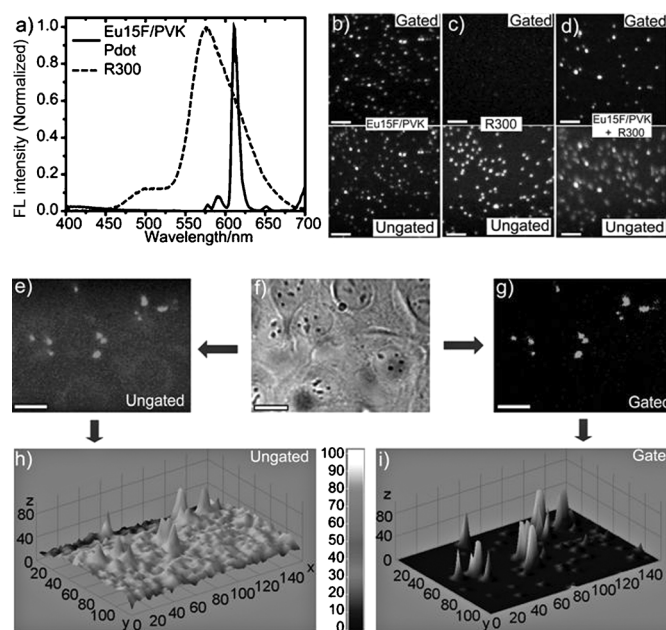


Figure 3. The application of the long luminescence lifetime of Eu complex/PVK Pdots in particle differentiation and cell imaging. a) Emission spectra of Eu15F/PVK Pdots and R300 nanoparticles (excited at 342 nm). b–d) Time-gated and ungated single-particle images of Eu15F/PVK Pdots, R300 nanoparticles, and mixtures of Eu15F/PVK Pdots and R300 nanoparticles; scale bar represents 5 μm . e) Ungated fluorescence microscopy image, f) bright-field microscopy image, and g) time-gated fluorescence microscopy image of unconjugated Eu15F/PVK Pdots inside MCF-7 cells; scale bar represents 50 μm . h, i) The interactive 3D surface plot of ungated image (e) and gated image (g).

nanoparticles could not be differentiated by using a band-pass filter when the mixture was imaged under a normal epifluorescence microscope (Figure 3d, lower image). But time-gated fluorescence microscopy allowed them to be easily differentiated (Figure 3d, top image). The delay time, between the termination of excitation illumination and start of fluorescence signal collection, of the time-gated microscope was set to be shorter than the lifetime of Eu15F/PVK Pdots but longer than that of R300 NPs. In this setup, only the Eu15F/PVK Pdots could be imaged, because they still emitted photons after the delay time (Figure 3b); the R300 NPs failed to emit photons after the delay time because of their short lifetime (3.6 ns) (Figure 3c). With this approach, two different types of nanoparticles with overlapping emission spectra were

successfully differentiated by exploiting their luminescence lifetime difference.

The long luminescence lifetime of the Eu15F/PVK Pdots also can be applied to improve the S/N ratio in cell imaging. For example, time-gated and ungated microscopy images of MCF-7 cells with internalized Eu15F/PVK Pdots were collected (Figure 3e–i). The background fluorescence intensity in the time-gated fluorescence cell images (Figure 3g,i) was much lower than in the ungated images (Figure 3e,h). This was because the lifetime of cellular autofluorescence, generated by molecules such as nicotinamide adenine dinucleotide, riboflavin, and flavin coenzymes, is in the order of nanoseconds,^[26] which can be efficiently filtered out in a time-gated microscope. As a result, the S/N ratio of cell imaging was successfully improved, from 85 to 232.

In summary, we designed and prepared Eu complex/PVK Pdots, which are a new type of Pdots with ultranarrow fluorescence emission with 8 nm FWHM; greatly decreased self-quenching of the Eu complexes; highly improved luminescence QY; and long fluorescence lifetimes. The bioconjugated Eu complex/Pdots were successfully used to label cellular components. The long lifetimes of the Eu complex/Pdots helped to distinguish them from other red fluorescence emitting nanoparticles and to improve the S/N ratio in imaging. We believe that the Eu complex/PVK Pdots may also find applications in imaging other specimens, such as biological tissues, which usually have high autofluorescence background signals.

Experimental Section

Poly(9-vinylcarbazole) (PVK, MW 50000 Da) was purchased from Sigma–Aldrich (St. Louis, MO, USA). Polystyrene-grafted poly(ethylene glycol) functionalized with carboxyl groups (PS-PEG-COOH) was purchased from Polymer Source Inc. (Quebec, Canada). Europium complexes Eu15F and EuDNM were synthesized as reported earlier.^[15,27] 300 nm Nanoparticles with red fluorescence (R300 NPs) were purchased from Thermo Scientific (IL, USA). Eu complex/PVK Pdot preparation, conjugation, and flow cytometry experiments are described in more detail in the Supporting Information.

The absorption and fluorescence spectra were measured with a DU 720 scanning spectrophotometer (Beckman Coulter, Inc., CA) and a Fluorolog-3 fluorospectrometer (HORIBA JobinYvon, NJ, USA). Fluorescence QYs were collected using an integrating sphere (model C9920-02, Hamamatsu Photonics). The luminescence lifetime data of PVK Pdots and PVK Pdots doped with Eu complex were obtained with a Lecroy Wave Runner 6100 digital oscilloscope (1 GHz) using the excitation of a third harmonic (355 nm) of a Nd:YAG laser (pulse width of 6 ns).^[27] The lifetime of R300 NPs was measured by using a PicoQuant Fluorescence lifetime system (PicoQuant Photonics North America Inc. Westfield, MA USA).^[6]

A Nikon TE2000 inverted microscope was modified for time-gated fluorescence image collection. Instrumentation details are described in the Supporting Information.

Received: June 4, 2013

Revised: July 29, 2013

Published online: September 12, 2013

Keywords: europium · fluorescence · imaging agents · polymer dots

- [1] C. Wu, D. T. Chiu, *Angew. Chem.* **2013**, *125*, 3164; *Angew. Chem. Int. Ed.* **2013**, *52*, 3086.
- [2] Y. Rong, C. Wu, J. Yu, X. Zhang, F. Ye, M. Zeigler, M. E. Gallina, I. C. Wu, Y. Zhang, Y.-H. Chan, W. Sun, K. Uvdal, D. T. Chiu, *ACS Nano* **2013**, *7*, 376.
- [3] Z. Tian, J. Yu, X. Wang, L. C. Groff, J. L. Grimland, J. D. McNeill, *J. Phys. Chem. B* **2012**, *116*, 4517.
- [4] J. Yu, C. Wu, S. P. Sahu, L. P. Fernando, C. Szymanski, J. McNeill, *J. Am. Chem. Soc.* **2009**, *131*, 18410.
- [5] J. Yu, C. Wu, Z. Tian, J. McNeill, *Nano Lett.* **2012**, *12*, 1300.
- [6] X. Zhang, J. Yu, Y. Rong, F. Ye, D. T. Chiu, K. Uvdal, *Chem. Sci.* **2013**, *4*, 2143.
- [7] J. B. Yu, C. F. Wu, X. J. Zhang, F. M. Ye, M. E. Gallina, Y. Rong, I. C. Wu, W. Sun, Y. H. Chan, D. T. Chiu, *Adv. Mater.* **2012**, *24*, 3498.
- [8] C. F. Wu, S. J. Hansen, Q. O. Hou, J. B. Yu, M. Zeigler, Y. H. Jin, D. R. Burnham, J. D. McNeill, J. M. Olson, D. T. Chiu, *Angew. Chem.* **2011**, *123*, 3492; *Angew. Chem. Int. Ed.* **2011**, *50*, 3430.
- [9] J. Yu, L. Zhou, H. Zhang, Y. Zheng, H. Li, R. Deng, Z. Peng, Z. Li, *Inorg. Chem.* **2005**, *44*, 1611.
- [10] J.-C. G. Bünzli, *Chem. Rev.* **2010**, *110*, 2729.
- [11] L. D. Carlos, R. A. S. Ferreira, V. D. Bermudez, B. Julian-Lopez, P. Escribano, *Chem. Soc. Rev.* **2011**, *40*, 536.
- [12] Y. Ma, Y. Wang, *Coord. Chem. Rev.* **2010**, *254*, 972.
- [13] S. V. Eliseeva, J.-C. G. Bünzli, *Chem. Soc. Rev.* **2010**, *39*, 189.
- [14] K. Binnemans, *Chem. Rev.* **2009**, *109*, 4283.
- [15] H. Peng, M. I. J. Stich, J. Yu, L.-n. Sun, L. H. Fischer, O. S. Wolfbeis, *Adv. Mater.* **2010**, *22*, 716.
- [16] K. Ai, B. Zhang, L. Lu, *Angew. Chem.* **2009**, *121*, 310; *Angew. Chem. Int. Ed.* **2009**, *48*, 304.
- [17] D. B. Ambili Raj, S. Biju, M. L. P. Reddy, *J. Mater. Chem.* **2009**, *19*, 7976.
- [18] C. Philippot, A. Bourdolle, O. Maury, F. Dubois, B. Boury, S. Brustlein, S. Brasselet, C. Andraud, A. Ibanez, *J. Mater. Chem.* **2011**, *21*, 18613.
- [19] A. P. Duarte, M. Gressier, M.-J. Menu, J. Dexpert-Ghys, J. M. A. Caiut, S. J. L. Ribeiro, *J. Phys. Chem. C* **2012**, *116*, 505.
- [20] N. Wartenberg, O. Raccurt, D. Imbert, M. Mazzanti, E. Bourgeat-Lami, *J. Mater. Chem. C* **2013**, *1*, 2061.
- [21] Y. H. Jin, F. M. Ye, M. Zeigler, C. F. Wu, D. T. Chiu, *ACS Nano* **2011**, *5*, 1468.
- [22] C. F. Wu, B. Bull, K. Christensen, J. McNeill, *Angew. Chem.* **2009**, *121*, 2779; *Angew. Chem. Int. Ed.* **2009**, *48*, 2741.
- [23] W. Sun, S. Hayden, Y. H. Jin, Y. Rong, J. B. Yu, F. M. Ye, Y. H. Chan, M. Zeigler, C. F. Wu, D. T. Chiu, *Nanoscale* **2012**, *4*, 7246.
- [24] C. Wu, B. Bull, C. Szymanski, K. Christensen, J. McNeill, *ACS Nano* **2008**, *2*, 2415.
- [25] X. Zhang, J. Yu, C. Wu, Y. Jin, Y. Rong, F. Ye, D. T. Chiu, *ACS Nano* **2012**, *6*, 5429.
- [26] J. E. Aubin, *J. Histochem. Cytochem.* **1979**, *27*, 36.
- [27] J. B. Yu, R. P. Deng, L. N. Sun, Z. F. Li, H. J. Zhang, *J. Lumin.* **2011**, *131*, 328.